GEOPHYSICS, VOL. 57, NO. 1 (JANUARY 1992); P. 136–145, 11 FIGS.

Nonlinear seismic trace interpolation

Douglas G. Martinson* and John R. Hopper*

ABSTRACT

The nonlinear correlation technique has been used to guide a seismic trace interpolant to fill gaps in seismic surveys, replace noisy traces, and produce evenly spaced arrays. Given an initial alignment (NMO correction for prestack data and manually inserted correlation lines for post-stack data), the correlation aligns corresponding features between adjacent seismic traces and quantifies the traveltime difference between the traces on a point-for-point basis. This information is used to construct synthetic (interpolated) traces, at any arbitrary distance between the correlated traces, which preserve dip and amplitude changes of the individual reflectors, assuming that such dip and amplitude changes occur linearly (or some other specified functional form) between the correlated traces.

The technique is applied to a 48-channel, NMO corrected, CDP gather and to a stacked seismic section to demonstrate its use, sensitivities, and limitations in processing and geologic interpretation studies. Traces synthesized in the CDP gather filling an artificial gap 0.85 km wide reproduce the true traces from the gap with good fidelity (correlation coefficients between the synthetic and real traces average ≥ 0.85). In another example, ~85 percent of the variance of the original 48-channel CDP gather is recovered through interpolation by using only 16 channels. A stacked section, with true trace spacing of 25 m, was decimated to 100 m trace spacing, then interpolated to restore the original 25 m spacing. The interpolated traces reproduce the real traces with correlations of ≥ 0.95, thus recovering ≥ 90 percent of the variance of the original section.

INTRODUCTION

Variable operating conditions during seismic surveys on land and at sea frequently result in noisy traces, gaps in coverage, and irregular or inadequate (with respect to spatial aliasing) trace spacing. These problems can limit or degrade data processing and hinder geological interpretation. While techniques exist that can overcome or circumvent some of the problems (e.g., transformation to the intercept-slowness, τ-p, domain for prestack data), trace interpolation in the space-time (x-t) domain can be used to overcome many of the spatial sampling problems in both prestack and stacked data. Trace interpolation in x-t is inherently nonlinear, and as suggested by Larner et al. (1981) and later derived by Bardan (1987), is most easily addressed through two distinct steps: (1) dip alignment, followed by, (2) simple interpolation along the dips. In this manner, assuming the correct dip alignments are introduced, the standard rectangular sampling lattice (time-space) responsible for introducing spatial aliasing of dipping events is replaced by the appropriate nonrectangular time-dip lattice. This extends spatial wavenumbers and eliminates aliasing introduced by the slope of dipping events (Bardan, 1987); although aliasing associated with dip curvature between traces is not eliminated by dip alignment.

The fidelity of the trace interpolation is highly sensitive to the accuracy with which the dips are determined, or the seismic events aligned, before interpolating along the dips (Bardan, 1987; Miller and French, 1989; Kao et al., 1990). This dip alignment can be made in a variety of ways. Miller and French (1989), though not specific, suggest graphical input and a priori information from field measurements. Schneider and Backus (1968), Larner et al. (1981), Finn and Backus (1986), and Bardan (1987) essentially find the most coherent average dip over local windows. However, by limiting the dip to averages over local windows, or between constrained levels, the methods are limited in their ability to resolve changes in dip as a function of time. Finn and Backus (1986) also suggest a method of "time warping," but details are not provided.

Manuscript received by the Editor November 6, 1990; revised manuscript received August 8, 1991.
*Lamont-Doherty Geological Observatory and Department of Geological Sciences, Columbia University, Palisades, NY 10964.

In this paper, we present a method of seismic trace interpolation using the nonlinear correlation technique of Martinson et al. (1982) in which the dip alignment is allowed to vary continuously in time. This correlation technique establishes a point-for-point correlation between traces providing a precise dip alignment at all time levels. The interpolation method is applicable in a data-dependent manner. It preserves amplitude and bandwidth, and has a wide range of applications. We use the phrase "nonlinear" to describe this method simply to emphasize the use of the nonlinear correlation and to distinguish this approach from those which rely on linear alignments over local windows or between discrete levels. Here, we present the method, given both pre- and post-stack applications, discuss practical aspects, and compare it to other interpolation schemes.

OVERVIEW OF NONLINEAR CORRELATION METHOD

The technique

Following Martinson et al. (1982), assume that two seismic traces to be correlated, $u(x = x_1, t)$ and $u(x = x_2, t)$ (x_i = receiver point; t = time), are similar except that one has undergone a stretching and/or squeezing of its time axis relative to that of the other. This "distortion" can be described by a mapping function $T(x_1, x_2, t')$ of unknown shape, which relates features in one trace at times $t = t'$ to the corresponding features in the other at times $t = T$ (Figure 1). Martinson et al. (1982) parameterize the mapping function as a linear trend modified by a truncated Fourier sine series with unknown coefficients, a_i. The method seeks to find those coefficient values that produce a mapping function whose shape maximizes a correlation coefficient (or coherence) C, describing the degree of similarity between the two traces. The value of C is thus dependent upon the values of the mapping function coefficients. Where the values produce the best correlation, C is at its maximum, and all $\partial C/\partial a_i$, in the gradient vector $\nabla \mathbf{C}(a_i)$, are zero.

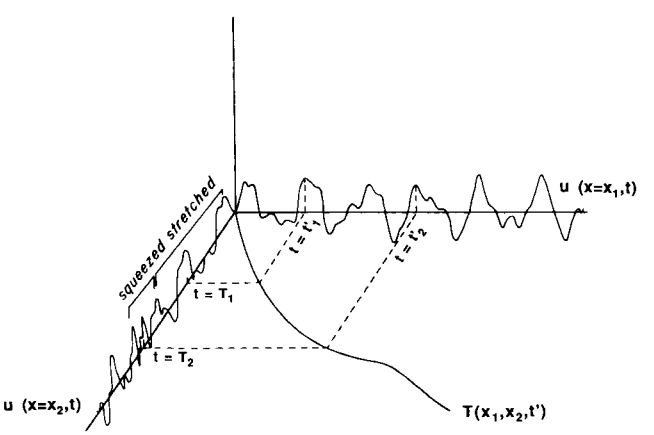

FIG. 1. Schematic showing how the mapping function $T(x_1, x_2, t')$ relates corresponding features between two traces, $u(x = x_1, t)$ and $u(x = x_2, t)$, being correlated.

A linear inverse approach is used in an iterative manner to determine the a_i coefficients that maximize the correlation. A small improvement in C, ΔC, is realized by changing the coefficients by a small amount, Δa_i, so $\Delta C = \nabla \mathbf{C} \cdot \Delta \mathbf{a}$. This provides one constraint on the values of Δa_i. The other constraints are obtained by requiring that the increments $\Delta \mathbf{a}$ are always in the direction in which $C(a_i)$ is increasing most rapidly, so $\nabla \mathbf{C}$ must parallel $\Delta \mathbf{a}$, or $\Delta \mathbf{a} = \beta \nabla \mathbf{C}$. These constraints allow for the solution of $\Delta \mathbf{a}$, the details of which can be found in Martinson et al. (1982).

The method starts from some initial position on $C(a_i)$; that is, from some initial estimate of alignment between the traces being correlated. It then proceeds iteratively to make small changes in the coefficients a_i until $|\nabla \mathbf{C}| = 0$, which represents a maximum correlation—within the general vicinity of the initial alignment (this point is discussed in more detail in the following section). The solution produces a correlation that minimizes (locally or globally) the least-squared error between the two traces as a function of the mapping function coefficients (see Martinson et al., 1982).

Implementation considerations

Initial estimate— The result obtained using this method can be sensitive to the initial alignment of the traces (see Martinson et al., 1982, for a complete discussion). The method produces the best correlation by making adjustments over a limited region, prescribed by the lowest frequency component of the mapping function. If the initial estimate is poor, the method may converge to a local maximum. Often, an acceptable initial estimate is achieved by simply aligning the ends of the traces to be correlated. For large separation distances or for traces with significant distortion, a better initial estimate is required. This can be obtained through insertion of manually picked correlation lines that correlate known features in the traces, or by using any of the dip alignment methods discussed in the Introduction.

For CDP gathers, a satisfactory initial estimate is usually obtained by making a standard NMO correction derived from conventional hyperbolic semblance analysis. For post-stack data, the choice of initial alignment can be more difficult. If the traces cannot be aligned initially to some acceptable degree (visual or otherwise) using correlation lines, then this technique will not necessarily produce the uniquely "correct" correlation. Note, however, that the automation provided by the technique does allow quick evaluation of a number of different correlations (using different initial alignments) which may help with difficult cases.

Correlation Resolution— In general, the number of coefficients defining the mapping function dictates the resolution (wavelength) at which distortions are eliminated. Each coefficient corresponds to a half harmonic in the mapping function, the higher coefficients corresponding to the higher frequency harmonics. Increasing the number of coefficients allows higher frequency information to be described by the mapping function and shorter wavelength distortions can be resolved. The resolution is limited by the shortest resolvable wavelength, which is given as the length scale $L = T/(n - 1)$, where T is the trace time span and n is the number of coefficients used. For example, if 101 coefficients are used to define the mapping function, stretching/squeezing at length

scales as short as 0.01 of the total length of the trace are generally resolved. If a wavelet has a width that is greater than this, then the mapping function allows small scale correlations that can introduce a stretching/squeezing of the wavelet shape itself.

Because of the modification of the Fourier sine series in the mapping function by a linear trend (which has a continuous Fourier transform), wavelengths shorter than those defined by L are actually resolved by the mapping function. That is, the mapping function can contain a variety of sharp bends (high curvature) and steep or shallow slopes that resolve short wavelength distortions ($<L$) locally, but as a general rule, the continuous overall resolution is limited by the highest frequency component of the mapping function.

The resolution to which the correlation should be carried out, is application-dependent. For geologic interpretation of stacked seismic sections, it is important to avoid artificial pulse distortion. Thus, the number of mapping function coefficients n is chosen so that $L \gtrsim L_w$, where L_w is the width of a typical wavelet. With prestack applications, correlations are commonly performed on NMO corrected CDP gathers. This correction introduces a stretching of the seismic pulse that can be severe at large source-receiver offsets (Dunkin and Levin, 1973). To account for this, n is chosen so that $L_w \leq L \leq L_D$ where L_w is the width of the undistorted seismic wavelet and L_D is the width of the stretched wavelet.

INTERPOLATION SCHEME

The ability to interpolate through the nonlinear correlation requires consideration of the mapping function. Consider the bold traces in Figure 2 (CDP-7 and CDP-12) which occur on two sides of a gap in a seismic section. After examining the entire seismic section, two correlation lines were imposed (Figure 2), and CDP-7 and CDP-12 were then correlated. The resulting mapping function indicates, for example, that the reflector in CDP-7 at a depth of ~600 ft (~200 m) dips downward across the gap and corresponds to a reflector of reduced amplitude in CDP-12 at ~625 ft (~190 m). This information is used to produce an interpolated representation of this reflector across the gap that preserves both the downward dip and gradual amplitude decay. The assumptions involved are that the coherent seismic events are properly correlated, and that the amplitude decay of an individual reflector, and its dip, vary linearly or with some other specified functional form across the gap (consistent with Bardan, 1987). Doing this for every mapped point of the two traces allows construction of interpolated traces at any desired spacing that preserves both the structure (move-out or dip) and amplitude changes of the individual reflectors.

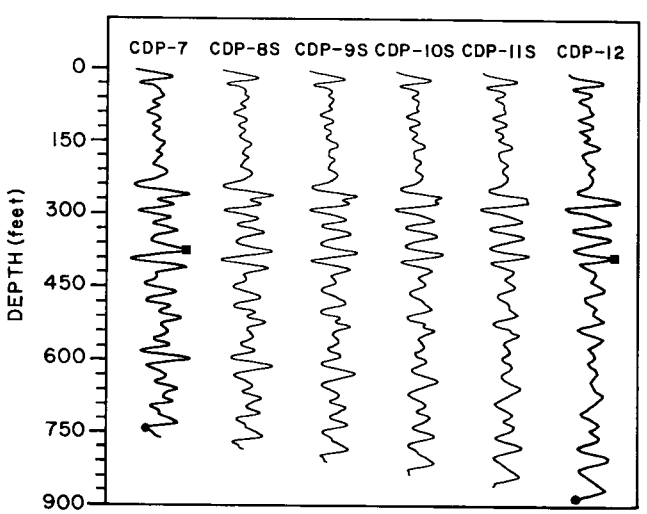

FIG. 2. Example of four interpolated seismic traces (CDP-8S, 9S, 10S, 11S) across a gap in a seismic section using the nonlinear interpolant. The recorded traces CDP-7 and CDP-12 (bold), which border the gap, were correlated to guide the interpolation. The correlation was aided by initially aligning the two points indicated by the squares and the circles on the recorded traces.

Specifically, if $T(x_i, x_{i+1}, t')$ is the mapping function correlating two neighboring traces, at receiver points x_i and x_{i+1} in the seismic wavefield $u(x, t)$ then:

$$u(x_i, t = t') = u[x_{i+1}, t = T(x_i, x_{i+1}, t')] + \varepsilon(x_i, x_{i+1}, t = T), \quad (1)$$

where $T(x_i, x_{i+1}, t')$ minimizes the error function $\varepsilon(x, t)$ in a least-squares sense.

The interpolant for $u(x, t)$ defined between any two sampled traces $x_i \leq x \leq x_{i+1}$ is given by:

$$u(x, t) = w_i u[x_i, t'(t)] + w_{i+1} u\{x_{i+1}, T[x_i, x_{i+1}, t'(t)]\}, \quad (2)$$

where: $w_i = (x_{i+1} - x)/\Delta x$; $w_{i+1} = (x - x_i)/\Delta x = 1 - w_i$; and $\Delta x = x_{i+1} - x_i$ is the distance between the sampled traces.

The time $t'(t)$ is given by solution of the implicit equation:

$$t'(t) = t - w_{i+1}\Delta t, \quad (3)$$

where $\Delta t = T[x_i, x_{i+1}, t'(t)] - t'(t)$ is the time displacement between the sampled traces for a given seismic event.

EXAMPLES

Prestack processing

Figure 3a shows a 48-channel CDP gather from the Exmouth Plateau (Mutter et al., 1989) with a nominal trace spacing of 50 m. We applied the NMO correction of Mutter et al. (1989) to the gather (Figure 3b), and performed all correlations and interpolations with these corrected traces. This serves two distinct purposes: (1) it eliminates the hyperbolic trajectory of the events across the gaps to be filled, so that simple linear interpolation along aligned dips will suffice; and, (2) it serves as the initial estimate to the mapping function. Most results are displayed with NMO correction, and unless otherwise noted, 50 mapping function coefficients are used to provide ~40 ms correlation resolution.

First, the method is used to create a synthetic version of the central trace, T-24 in Figure 3, by interpolation between the adjacent traces T-23 and T-25, which are separated

spatially by 100 m. As seen in Figure 4a, comparison of the synthetic (interpolated) trace S-24 (solid line) to the real trace T-24 (dotted line) shows an excellent agreement with a correlation of $C = 0.97$.

Sensitivity of the interpolant to separation distance between the correlated traces is tested by repeating this experiment using traces symmetrically distributed about T-24 but separated by greater and greater distances. The correlation coefficient drops off rapidly from values of ≥ 0.85 to ≤ 0.65 after a separation distance of 700 m (Figure 5, solid line). Over distances ≤ 700 m, the synthetic trace consistently provides an excellent approximation to the real trace; Figure 4b shows the result achieved at 700 m. Small-scale differences are seen but these are likely due to random noise in the traces. Over distances >700 m, the interpolant no longer reproduces the recorded trace (Figure 4c). This reflects the failure of the correlation due to the initial misalignment of reflectors at ≥ 2.5 s by the NMO correction used here as the initial estimate (demonstrated below). A better initial estimate before correlating the traces at these large separation distances may overcome such problems.

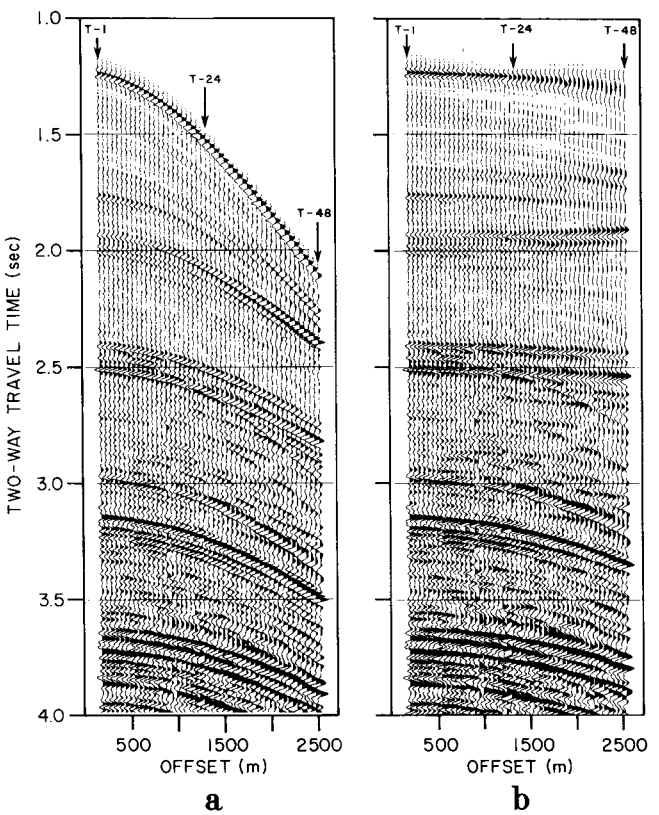

FIG. 3. 48-channel CDP gather from the Exmouth Plateau (Mutter et al., 1989) used to demonstrate the technique in this study. Total spatial offset is 2.4 km with 50 m trace spacing. Automatic gain control (AGC) has been applied for display purposes. For correlations, a spherical divergence correction was applied. (a) The gather prior to an NMO correction. (b) The gather after application of an NMO correction using the stacking velocities of Mutter et al. (1989). Key traces referred to in the text are labeled.

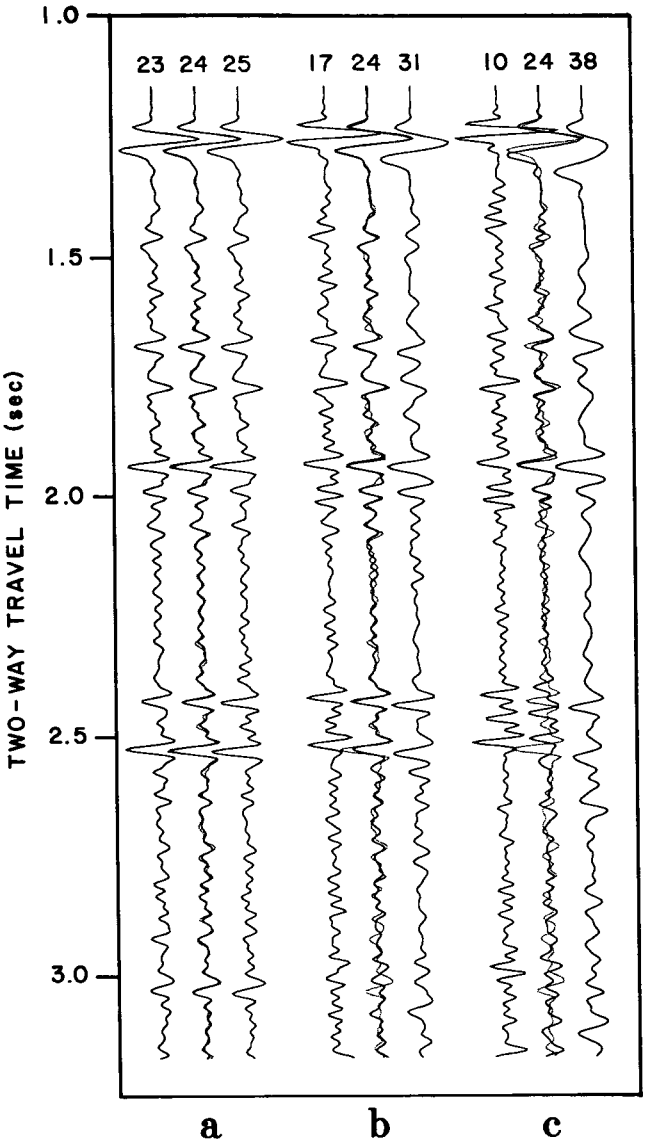

FIG. 4. Sensitivity of the interpolant to the separation distance between the traces correlated to guide the interpolation. In each panel, T-24 (the central trace of the CDP gather in Figure 3) has been synthesized by correlating traces symmetrically located on either side of it that are separated by increasing distances. The traces that were correlated are shown on either side of the synthetic trace (solid), which is superimposed on the recorded T-24 (dotted). The coherence C between the real trace and synthetic generated from each correlation is also given. (a) Correlating T-23 and T-25, separation distance of 100 m, $C = 0.97$. (b) Correlating T-17 and T-31, separation distance of 700 m, $C = 0.85$. (c) Correlating T-10 and T-38, separation distance of 1400 m, $C = 0.43$.

For this particular data set, noise is not a significant problem, as indicated by the excellent match between the real and synthetic traces. This match will be degraded as the signal-to-noise ratio decreases in the data, in which case better statistical stability can be obtained by averaging several independent synthetic traces. An example of this is shown in Figure 6, where four synthetic versions of T-24 were generated from eight different traces and then averaged. The coherence between the real and averaged synthetic trace is greater than the coherence between the real and any individual synthetic trace. This reflects a reduction of random (i.e., uncorrelated) noise due to the averaging process. Note that the coherent noise is aligned by the correlation and thus preserved in the interpolated traces; it can be removed in subsequent processing steps using methods such as 2-D filtering.

A second experiment tests the fidelity of an entire section of traces synthesized across an increasingly wider gap. This test generates synthetic traces to fill a gap between T-1 (Figure 3) and neighboring traces where the neighboring traces become increasingly farther away from T-1. Figure 7a shows a comparison between the 16 synthetic traces created between T-1 and T-18 and the real traces existing over this 0.85 km separation distance. The overall match is excellent with an average coherence, $\bar{C} = 0.85$. The principal difference between real and synthetic traces is the failure of the method to reproduce the multiple event at about 3.0 s (see Figure 3). This reflects a poor initial alignment of the multiple event by the NMO correction over this separation distance. For shorter separation distances, both primary and multiple energy are roughly aligned so that the interpolant captures both, improving the match and $\bar{C}$ (Figure 7b). The distance over which one can interpolate automatically is thus dependent on whether or not it is necessary for the interpolant to capture the coherent noise (multiples, diffracted energy, etc.) as desired for some *f-k* filtering applications.

The method is also dependent on the quality of the initial estimate. At separation distances greater than 0.85 km for this example, the method begins to break down. This is because the preliminary hyperbolic NMO correction applied here, which only approximates the true traveltime expression, no longer aligns the primary events at 2.5 s sufficiently to succeed (Figure 8). Inserting a single correlation line to better align this event allowed us to increase the separation distance to >1 km with $\bar{C} = 0.81$. Thus, a better initial estimate, either an improved NMO function or manually inserted tielines, is required to obtain satisfactory correlations over large separation distances.

Finally, the example of Figure 9 shows 4 seconds of a 48-channel CDP gather (Figure 9a) from the Exmouth Plateau (Mutter et al., 1989) with 50 m nominal trace spacing that has been decimated to 16 channels (Figure 9b) with a 150-m trace spacing. The Mutter et al. (1989) NMO correction was applied to the decimated gather and the traces correlated using 100 coefficients (~40 ms correlation resolution). Synthetic traces were interpolated to re-create the original 48-channel gather (Figure 9c), and the NMO correction was then removed. As seen by comparison of Figures 9a and 9c, the interpolation does an excellent job; $\bar{C} = 0.92$ indicating that the trace interpolation recovered ~85 percent of the variance in the original 48-channel gather using only 16 channels. The interpolated traces recover even the multiple, which interferes and crosses the reflectors at ~2.5 s and the spatial variation in the amplitudes of the reflectors centered at ~3.7 s. Figure 9d shows the result of interpolating further, to a 96-channel gather with 25 m trace spacing, which more clearly reveals the structure of the recorded events.

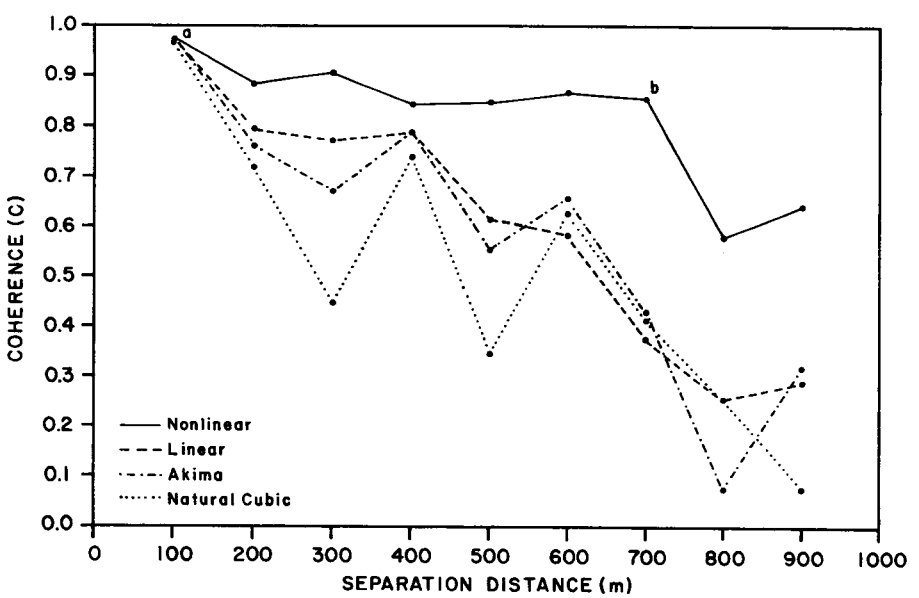

FIG. 5. Coherence between the synthetic (interpolated) version of T-24 and real T-24 (from Figure 3) as a function of the separation distance between the traces used for the interpolation (symmetrically distributed about T-24). The values corresponding to the separation distances of the examples from Figure 4 (a, b) are labeled. For comparison, the coherence is given for the present (nonlinear) interpolant as well as for three standard interpolants (linear, Akima's deficient spline and natural cubic spline).

Post-stack interpretation

For interpretation studies involving stacked seismic images, the separation distance over which the interpolant is valid is limited by the length scale over which the geologic structure is changing linearly (or analytically, given a different function). That is, the interpolant assumes each reflector dips linearly across the gap being interpolated, so significant deviations of the true dip from linearity will violate this assumption and introduce spatial aliasing, degrading the results. Also, the quality of the initial estimate required will vary as a function of the complexity of the geology and severity of initial misalignment. For difficult cases, given an absence of independent information, one can consider a variety of initial estimates (including a Monte Carlo approach) to extend the search for the global maximum correlation.

An example of the interpolant applied to a 2-D seismic section is given in Figure 10. The original 4 s section with 25 m trace spacing is shown in Figure 10a. This section was decimated by a factor of 4 (100 m trace spacing; Figure 10b), and this decimated section was then interpolated (~40 ms correlation resolution) to synthesize the original 25 m trace spacing. The correlation lines used for the initial estimate are shown in the Figure 10b insert. As seen, the interpolated section (Figure 10c) does an excellent job of reproducing the original section including the major regional uncomformity at ~3.1 s and some of the fault structure seen in the original data. Correlation coefficients between the synthetic and real traces are consistently >0.95. However, increasing the trace spacing results in undersampling the short spatial wavelength geology, which cannot be recovered by interpolation. Consequently, the interpolated section appears somewhat smoother than the original section (though >90 percent of the variance of the original traces has been recovered).

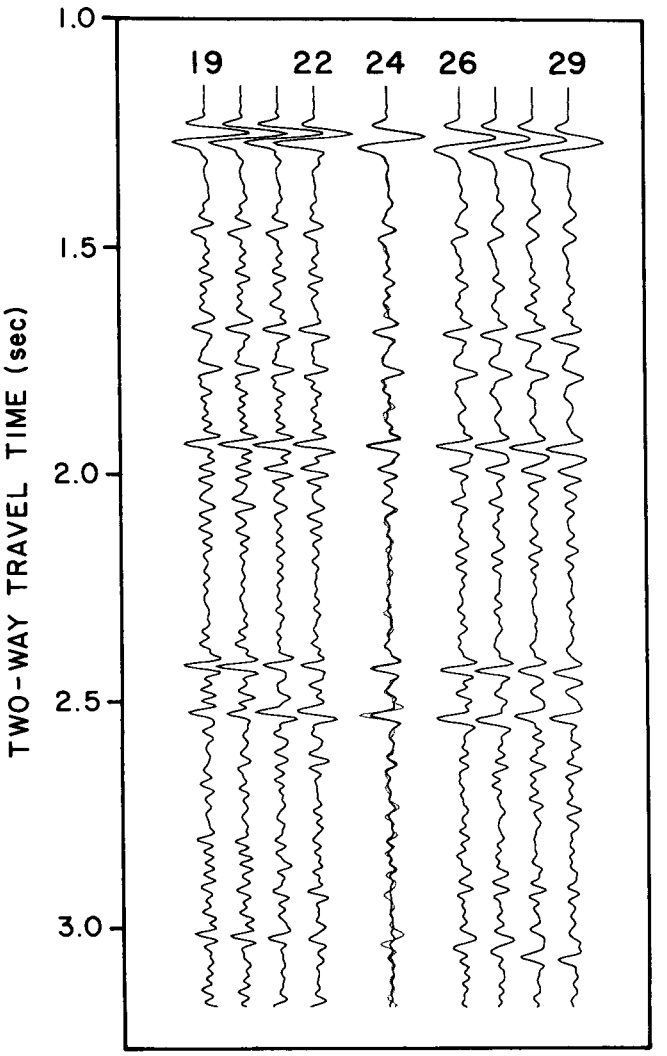

FIG. 6. Four synthesized versions of T-24 (from Figure 3) were averaged to produce a statistically stable synthetic T-24 shown (solid) superimposed on the recorded T-24 (dotted). The traces used to generate the four synthetic versions are shown (the coherence C between the recorded T-24 and the synthetic generated from each correlation is also given): T-22 was correlated with T-26 (C = 0.89); T-21 with T-27 (C = 0.91); T-20 and T-28 (C = 0.84); and T-19 with T-29 (C = 0.85). The averaged synthetic T-24 shows a stronger correlation to the real T-24 than any of the four individual synthetic traces do (C_{ave} = 0.92) due to the averaging.

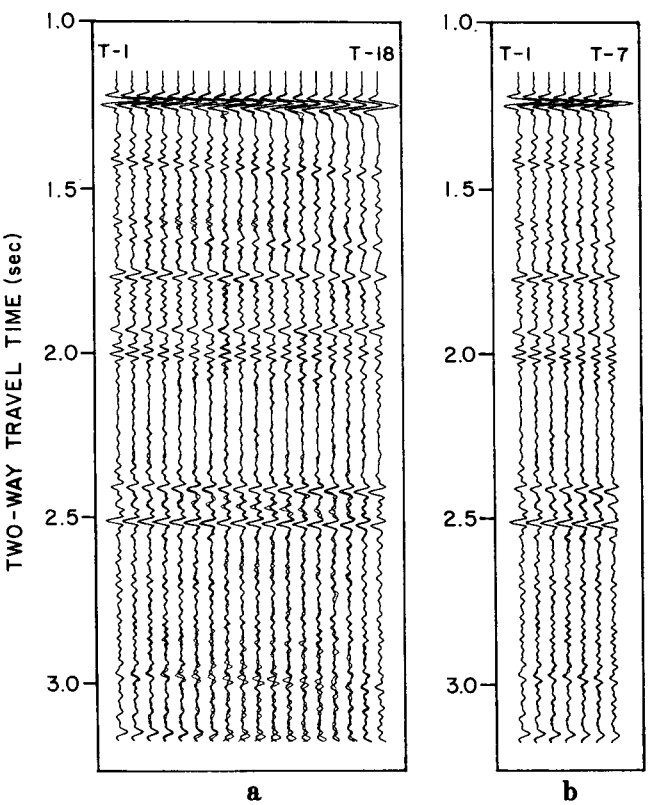

FIG. 7. Interpolation of a section of traces. Synthetic traces (solid) are superimposed on the real traces (dotted) which fill a gap between: (a) the real traces T-1 and T-18 (from Figure 3), and (b) T-1 and T-7.

PRACTICAL CONSIDERATIONS AND SENSITIVITIES

Sensitivity to correlation resolution

In the examples involving the data of Figure 3, the mapping functions were limited to 50 coefficients, implying a correlation resolution of ~40 ms over the 2 s sections. The traces are sampled at Δt = 4 ms, giving 10 data points per degree of freedom in the mapping function which provides a stable solution. Also, the correlation resolution is comparable to the typical seismic wavelet width in the traces which minimizes pulse distortion or "overtuning."

The interpolation results are relatively insensitive to the correlation resolution. Consider the generation of trace T-24 (Figure 3) by interpolation using traces T-21 and T-27. For ~20 ms correlation resolution (100 mapping function coefficients), the correlation between the interpolated and real trace T-24 gives C = 0.91; for ~40 ms resolution (50 coefficients), C = 0.91; and for ~80 ms resolution (25 coefficients), C = 0.90. This insensitivity indicates that distortions arising between neighboring traces occur over wavelengths of $\gtrsim$80 ms for this example. Higher correlation resolution, beyond that comparable to the wavelength of the distortion, accomplishes minimal change in the correlation due to the smooth nature of the seismic traces and minimal high-frequency noise contamination.

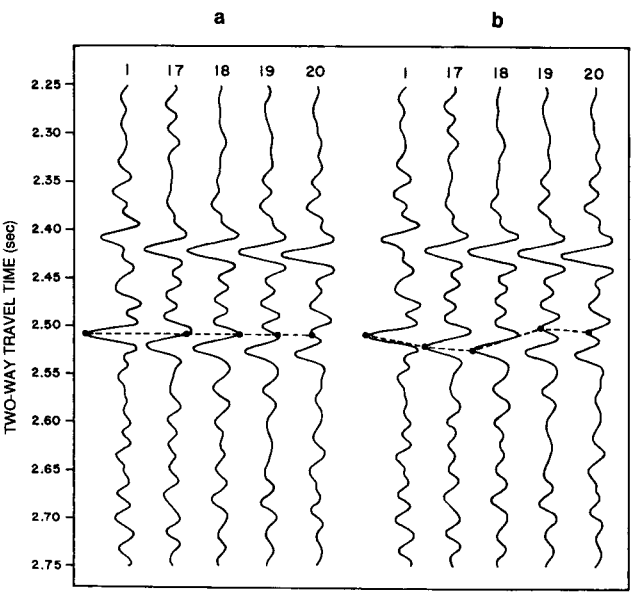

FIG. 8. (a) The alignment of the large reflector at 2.5 s in the CDP gather of Figure 3 after the NMO correction. Note that the correction is inaccurate so that by trace 20, the reflector is aligned with the wrong peak. This initial misalignment forces the miscorrelation shown by the dashed line in (b) and degrades the interpolant over these large separation distances. As seen in (b), the reflector is still properly correlated out to trace 18 which is why the interpolated section of Figure 7a is so good.

Comparison to other interpolants

Most methods previously used for aligning seismic events or determining dips prior to interpolation are limited in their ability to resolve changes in dip between neighboring events. The extreme sensitivity of seismic trace interpolation to the accuracy of dip determination, as suggested by Bardan (1987), Miller and French (1989) and Kao et al. (1990) is demonstrated here by a simple example. By subjecting the CDP gather of Figure 3 to the NMO correction of Mutter et al. (1989), we are in effect using a model-based alignment that maximizes a group-coherence (semblance) over local time windows. By using this NMO correction unmodified by nonlinear correlation as a dip alignment for interpolation, we can assess the sensitivity of trace interpolation to how well correlative features are aligned.

Figure 11a presents the result of repeating the example of Figure 4b, but synthesizing trace T-24 using only the NMO correction for the dip alignment. Most significant is the mismatch between the interpolated and recorded sea floor reflection (at ~1.25 s). A significant error is introduced as a consequence of the difference in the shape of the wavelet at this time horizon. That is, a single dip for the sea floor reflection is not sufficient to eliminate the offset-dependent pulse distortion. This reflects a sensitivity to very short timescale distortions that are not easily accounted for using window methods. As seen in Figure 4b, the nonlinear correlation eliminates this pulse distortion resulting in an excellent synthesis of the sea floor reflection. Also note that while the overall alignment between T-17 and T-31 in Figure 11a appears to be fairly good, the synthetic trace captures <20 percent of the variance of the recorded T-24, whereas in Figure 4b, the nonlinear method captures ~72 percent.

The coherence between the interpolated trace, generated using the NMO alignment, and the real trace as a function of increasing separation distance is shown by the dashed line (labeled "linear") in Figure 5. As seen, the method works well over a short distance (100 m representing a single missing trace), but drops off rapidly thereafter, again reflecting the sensitivity to the alignment. Because of this sensitivity, data-dependent methods should presumably fair better given noisy data.

Given an alignment of events, sensitivity to the form of the interpolant is low, though as with any interpolation, the actual interpolant used should reflect the physics or be consistent with a priori information regarding the behavior between recorded observations. Bardan (1987) suggests a simple linear interpolant (after dip alignment) which we have also used. For comparison, the results of Figure 11a are repeated using a deficient spline (Akima, 1970; Figure 11b) and a natural cubic spline (Figure 11c). Figure 5 shows for each interpolant the coherence between the real and synthesized traces as a function of the separation distance across the gap. While slight differences exist as expected, the overall difference is minor, suggesting the reduced sensitivity to the form of the interpolant provided that interpolation is performed along the line of dip at each time horizon. Kao et al. (1990) use a weighted interpolant that is not restricted to the dip line which may account for some of the amplitude degradation apparent in the interpolated traces in their Figure 5.

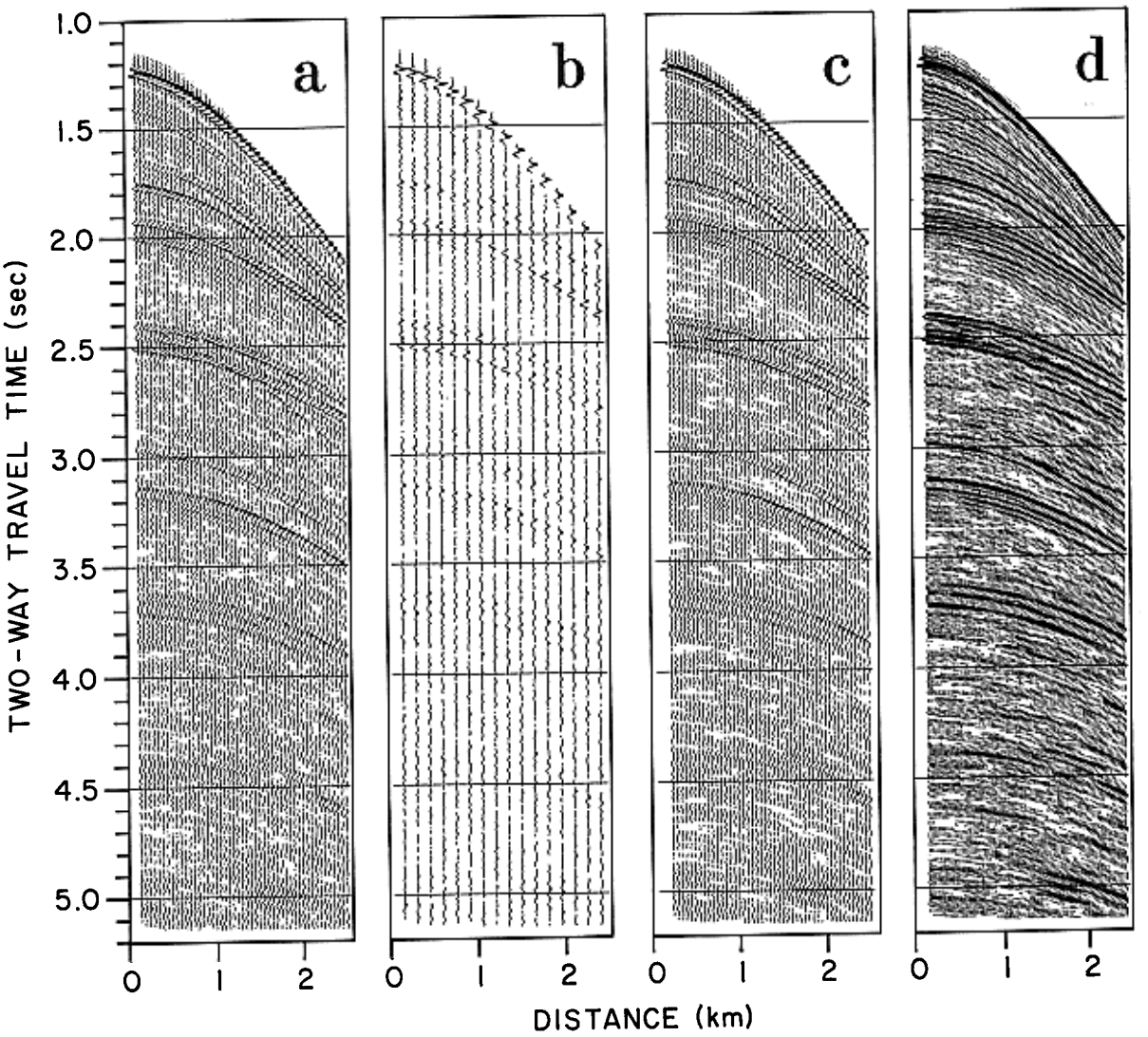

FIG. 9. (a) Four seconds of a 48-channel CDP gather from Exmouth Plateau (Mutter et al., 1989) with 50 m trace spacings. (b) Same as (a) only decimated to 16 channels, 150 m trace spacing. (c) Result of interpolating the decimated gather in (b) to produce a 48-channel gather simulating the original gather in (a). (d) Result of interpolating the decimated gather in (b) to produce a 96-channel gather, 25 m trace spacing.

Finally, other trace interpolation schemes involve the wave equation (Ronen, 1987), or τ-p transform, for prestack data only (e.g., Cabrera and Levy, 1984; Kappus et al., 1990). Ronen (1987) and Cabrera and Levy (1984) have met with limited success. Kappus et al. (1990) use the method of Henry et al. (1980) and obtained good results at short source-receiver offsets for individually eliminated traces. At large offsets (>1 km) they report unsatisfactory results. Note that these distances are absolute ranges, not total gap widths across which the interpolation was performed.

SUMMARY

Larner et al. (1980), Bardan (1987), Miller and French (1989), and Kao et al. (1990) have demonstrated and lauded the potential merits of seismic trace interpolation. Further, they have clearly indicated the sensitivity of trace interpolation to the accuracy of the dip alignment. In that regard, we have presented a technique that is well suited to address this sensitivity. Given an approximate initial alignment of the traces (such as NMO correction for prestack data, and manually inserted correlation lines for post-stack data), the technique automatically correlates the traces, generating a precise, point-for-point determination of the dip alignment. The technique appears to work well, it is computationally fast, and preserves amplitude and bandwidth of the interpolated traces.

By interpolating between existing traces, this method can be used to fill gaps in seismic data, replace noisy traces, produce evenly spaced arrays, and increase spatial density. For the NMO corrected CDP gather used here, the method accurately replicates the real traces eliminated to form a 0.85 km wide gap. In addition, the method appears to be relatively insensitive to absolute range (source-receiver offset). Range sensitivity is primarily a result of using hyperbolic NMO as an initial estimate to the mapping function, which works better at short ranges than at large ranges. In another example, ~85 percent of the variance of a 48-channel CDP gather is recovered by interpolation using only 16 of the original 48 channels.

For post-stack data, the technique can aid in the geologic interpretation of seismic sections by increasing the spatial density of the section, though short-wavelength geology not resolved by the spatial sampling cannot be recovered. For the example given, ≥90 percent of the variance of a seismic section is recovered when the method is used to increase the trace spacing from 100 m to 25 m. Care must be used with post-stack traces since the interpolation is sensitive to the initial alignment. However, the method can easily be implemented in an interactive way, and the choice of correlated horizons on a seismic section can be quickly evaluated.

Further applications of this interpolation method, such as conversion from 2-D seismic lines to 3-D data volumes, may

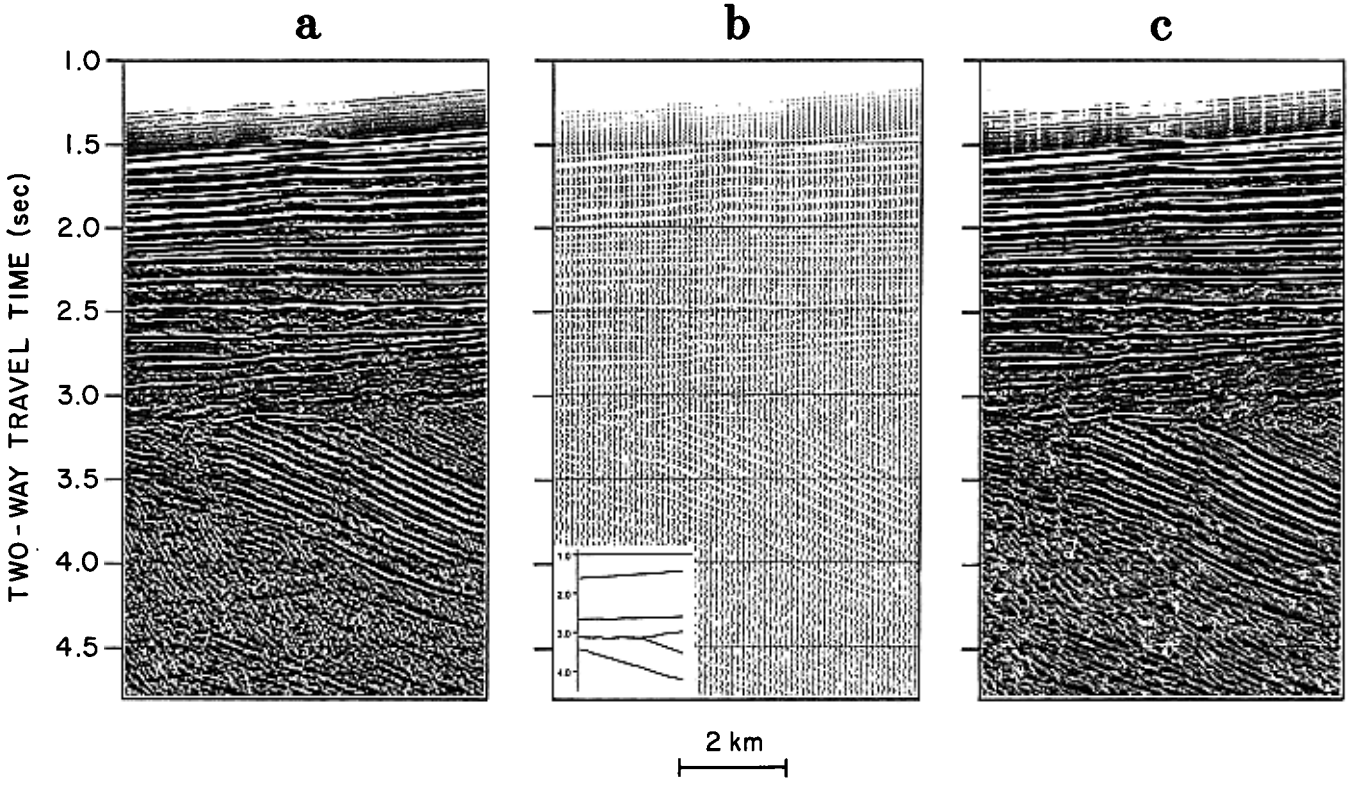

FIG. 10. Example of applying the interpolation to a stacked seismic section. (a) Original section with 25 m trace spacing. (b) Decimated section to 100 m spacing. (c) Synthesis of original section from the decimated section in (b). Insert shows correlation lines imposed initially to guide correlation.

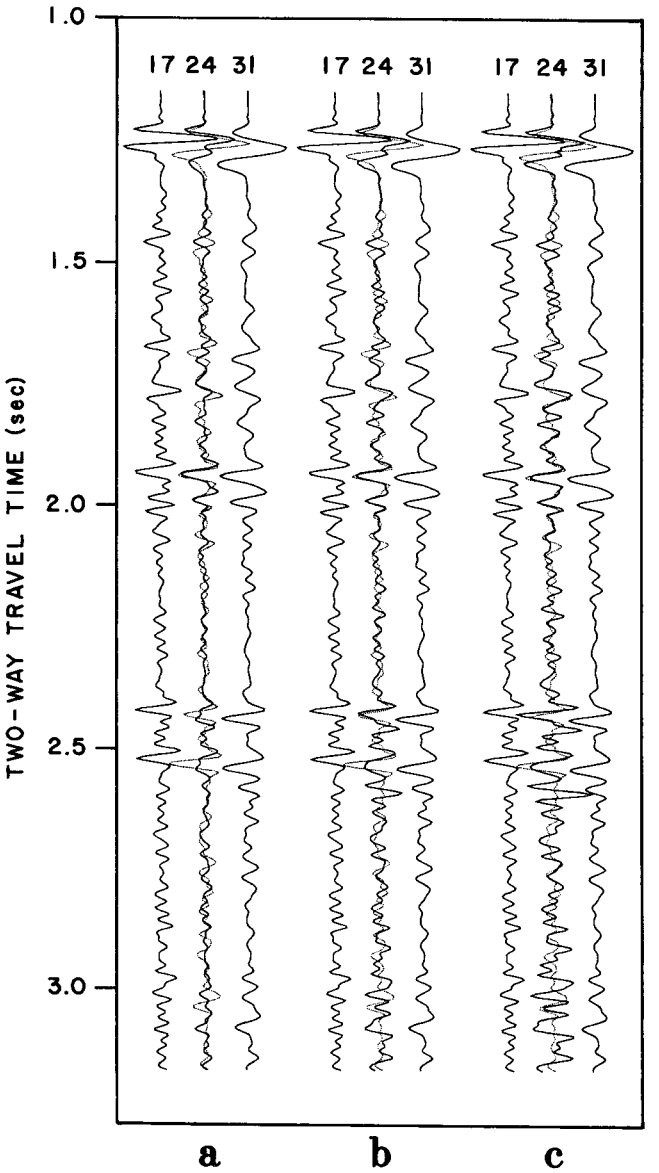

FIG. 11. Identical to Figure 4b, except in this case, the synthetic T-24 was generated by interpolating T-17 with T-31 using: (a) linear interpolant (coherence between the synthetic and recorded T-24, $C = 0.37$); (b) Akima's spline ($C = 0.41$); and (c) natural cubic spline ($C = 0.43$).

be possible. Despite obvious limitations, Miller and French (1989) and Kao et al. (1990) have demonstrated the benefits of using simple trace interpolation to successfully accomplish this conversion in practice, yielding tremendous benefits in both interpretation capabilities and field costs.

ACKNOWLEDGMENTS

This paper benefited from discussions with J. Mutter, W. Menke, A. Lerner-Lam, W. Bangs, C. Zehnder, P. Buhl, and J. Diebold. Computations were done using the commercial software package CORPAC© (which employs a computationally efficient scheme for implementing the Martinson et al., 1982, correlation method), distributed by GLOBEX LTD, P.O. Box 329, West Nyack, NY, 10994. The research was supported by National Science Foundation grant number OCE88-02760. Lamont-Doherty Geological Observatory contribution number 4806.

REFERENCES

Akima, H., 1970, A new method of interpolation and smooth curve fitting based on local procedures: J. Assoc. Comput. Mach., **17**, 589–602.

Bardan, V., 1987, Trace interpolation in seismic data processing: Geophys. Prosp., **35**, 343–358.

Cabrera, J. J., and Levy, S., 1984, Stable plane-wave decomposition and spherical-wave reconstruction: Applications to converted *S*-mode separation and trace interpolation: Geophysics, **49**, 1915–1932.

Dunkin, J. W., and Levin, F. R., 1973, Effect of normal moveout on a seismic pulse: Geophysics, **33**, 399–411.

Finn, C. J., and Backus, M. M., 1986, Estimation of three-dimensional dip and curvature from reflection seismic data: 56th Ann. Internat. Mtg., Soc. Expl. Geophys., Expanded Abstracts, 355–358.

Henry, M., Orcutt, J. A., and Parker, R. L., 1980, A new method for slant stacking refraction data: Geophys. Res. Lett., **7**, 1073–1076.

Kao, J. C-S, Schneider, W. A., and Whitman, W. W., 1990, Automated interpolation of two-dimensional seismic grids into three-dimensional data volume: Geophysics, **55**, 433–442.

Kappus, M. E., Harding, A. J., and Orcutt, J. A., 1990, A comparison of tau-*p* transform methods: Geophysics, **55**, 1202–1215.

Larner, K., Gibson, B., and Rothman, D., 1981, Trace interpolation and the design of seismic surveys: Geophysics, **46**, 407.

Martinson, D. G., Menke, W., and Stoffa, P. L., 1982, An inverse approach to signal correlation: J. Geophys. Res., **87**, 4807–4818.

Miller, M. H., Jr., and French, W. S., 1989, Time slices from two-dimensional sesmic surveys: Geophysics, **54**, 13–22.

Mutter, J. C., Larson, R. L., and the Northwest Australia Study Group, 1989, Extension of the Exmouth Plateau, offshore northwestern Australia: Deep seismic reflection/refraction evidence for simple and pure shear mechanisms: Geology, **17**, 15–18.

Ronen, J., 1987, Wave-equation trace interpolation: Geophysics, **52**, 973–984.

Schneider, W. A., and Backus, M. M., 1968, Dynamic correlation analysis: Geophysics, **33**, 105–126.